Original Article

Application of cone beam computed tomography in facial soft tissue thickness measurements for craniofacial reconstruction

Manasa Anand Meundi, Chaya Manoranjini David

Department of Oral Medicine and Radiology, Dayananda Sagar College of Dental Sciences, Bengaluru, Karnataka, India

Abstract

Context: The paradigm shift from two- to three-dimensional imaging has marked the beginning of a new era in diagnosis. Newly developed cone-beam computed tomography (CBCT) designed specifically to visualize maxillofacial pathologies is being used in forensic investigations also. Facial reconstruction is a specialized forensic technique to identify the deceased from the unknown skull. It is dependent on population-specific facial soft tissue thicknesses.

Aims: This study aims to propose the mean dataset of facial soft tissue thickness for South Indian population by utilizing CBCT. It also aims to evaluate the sex and racial differences in the values if any.

Settings and Design: This descriptive study was conducted on CBCT scans of South Indians.

Materials and Methods: Eighty CBCT scans of South Indian adults aged 18–80 years were selected. Facial soft tissue thickness measurements at 34 craniometric landmarks were carried out.

Statistical Analysis: Descriptive statistics was done. Student's t-test estimated the differences of soft tissue thickness between the sexes; bilateral measurements and also racial differences. Tukey's honest significant difference test was used for multiple comparisons among Indian studies.

Results: Males had thicker soft tissue than females in most of the landmarks. Differences in the bilateral soft tissue thicknesses were negligible. Indians had thicker facial tissues than the Koreans and CBCT was found efficient in measuring soft tissue thickness.

Conclusion: The present study provides facial soft tissue thickness dataset using CBCT which will be useful in forensic facial reconstructions of South Indian population as well as in maxillofacial and plastic reconstructive surgeries.

Keywords: Cone-beam computed tomography, facial reconstruction, facial soft tissue thickness, human identification, South India

INTRODUCTION

Diagnostic imaging is an important adjunct to clinical diagnosis of the patient. Intraoral and panoramic radiographs often fulfill the requirements of imaging hard tissues. However, these 2D radiographic methods have limited capabilities in the evaluation

Access this article online

Quick Response Code:

Website:
www.jomfp.in

DOI:
10.4103/jomfp.JOMFP_20_19

How to cite this article: Meundi MA, David CM. Application of cone beam computed tomography in facial soft tissue thickness measurements for craniofacial reconstruction. J Oral Maxillofac Pathol 2019;23:114-21.

of three-dimensional (3D) relationships. They also suffer from inherent limitations such as magnification and superimposition of structures.[1] Several imaging technologies such as computed tomography (CT) have now been successful in capturing the missing third dimension.[2]

CT images the subject by passing a fan-shaped X-ray beam to the detector through the patient lying within the rotating gantry. The sequential images acquired by scanning thin slices of body sections were being used extensively for diagnosing complex conditions such as craniofacial fractures, massive intraosseous tumors and others until the advent of cone-beam CT (CBCT) technology in the early 90s designed specifically for dentomaxillofacial imaging.

CBCT is the generation next that has emerged as a potentially low-dose volumetric imaging technique for visualizing maxillofacial structures, in which cone-shaped X-ray beam moves in a helical progression to acquire multiple individual image slices (approximately 150–800) as the X-ray source and the detector makes a single partial or complete circle around the patient.[3] Sequential, single-image captures are stacked as multiple offset lateral cephalograms, corrected, assembled and reconstructed using filtered back projection algorithm.[1,3] Further, secondary reconstructed images in the personal computer using dedicated software present the images to the radiologist in three orthogonal planes (axial, sagittal and coronal) and 3D reconstructions.[1,3]

Reduced physical footprint, a relatively low patient dose and its low cost have been responsible for the rapid uptake of CBCT in the dental health-care systems.[4] Apart from volumetric imaging, CBCT allows various nonaxial 2D images and synthesizes cephalograms comparable with the conventional ones.[5] Several such advantages have made CBCT useful in the diagnostic assessment of bony and dental pathologies including fractures, maxillofacial deformities, temporomandibular joint imaging and implant treatment planning; it also facilitates image-guided surgery.[3,4]

Radiography has been an integral part of forensic investigation ever since the discovery of X-ray in 1895.[6] Radiographic analyses have become a routine method in assessing biologic characteristics such as age and sex, in locating foreign objects such as projectiles and their wound paths, in evaluating fragmentary remains of the skull and other body parts. The ability of CT to depict the anatomic structures in 3D perspective has made it useful for performing noninvasive postmortem examinations such as virtopsies.[7,8] Apart from being smaller, CBCT offers several technical and practical advantages over conventional

CT that can easily replace for all forensic case purposes, especially when medical CTs are inaccessible.

Craniofacial reconstruction is a well-established but sparingly used forensic technique of predicting and recreating the face of the deceased over the skull to trigger individual identification.[9] Since its first attempt in the late 19th century, manual and computer-aided techniques have been developed,[10] both of which involve reconstructing the lost soft tissues under the guidance of soft tissue pegs placed at specific sites on the face that represent the average facial soft tissue thickness (FSTT).[10-12]

Since the contributions of renowned Russian anthropologist Mikhail Gerasimov, numerous studies have been undertaken to measure the average FSTT at specific sites on the face. On understanding the relationship of FSTT to age, sex, race and ethnicity, researchers have focused on establishing databases of FSTT for Caucasians, Germans, Japanese, Koreans and others.[12-15] However, studies providing soft tissue thickness for South Indian population are limited.

FSTT has been measured by both invasive and noninvasive methods. Historically, thin needles were probed into the cadaveric face at specific sites until they hit the bone surface and the depth of penetration was measured.[9,16] This invasive method was gradually overcome by several imaging-based methods including lateral cephalometric radiography,[17] ultrasound (USG),[13] magnetic resonance imaging (MRI)[18] and CT,[19] all of which have inherent advantages and limitations. While 2D lateral cephalometric radiographs are affected by magnification errors, additional landmarks cannot be incorporated at a later date in USG.[15] Both CT and MRI techniques are collected with patients in supine position causing gravity induced FSTT deformation. In addition, CT is limited by the health risks associated with radiation. Cone-beam CT scanner enables images to be obtained with the subject in an upright position at a lower radiation dose. The purpose of this study was to utilize CBCT for measurements of FSTT with an attempt to propose soft tissue thickness dataset for South Indian population. In addition, the study has attempted to analyze the efficiency of CBCT over other imaging techniques in the measurement of FSTT.

MATERIALS AND METHODS

This research was approved by the Institutional Review Board, Rajiv Gandhi University of Health Sciences, Bengaluru, India. CBCT images of 80 adults aged 18–80 years were randomly selected. Care was taken to exclude the scans of cases with swelling, trauma, facial deformities and those

under orthodontic treatment. The scans were obtained using CBCT scanner (Planmeca ProMax 3D Mid; Planmeca Oy; Helsinki, Finland) with a voxel size of 0.3–0.4 mm and a field of view of 20 cm × 17 cm. All the cases were scanned with their Frankfurt Horizontal (FH) plane parallel to the floor with teeth in occlusion. The resulting DICOM data were imported into OnDemand3D software (Cybermed, Seoul, Korea) in the personal computer to measure the distance between a point on the skull surface to the corresponding point on the soft tissue image which gives FSTT at the respective anatomical points. A total of 34 landmarks (12 midline and 11 pairs of bilateral) were chosen according to Stephan and Simpson[20] [Figure 1]. The landmarks on the skull surface were located on the reconstructed 3D image first, and the corresponding soft tissue landmark was identified using the preset hard and soft tissue display tool. Further, the identified points were accurately marked using two of the three orthogonal sections (coronal-axial or sagittal-axial) depending on the location of the landmarks.

Statistical analysis

General descriptive statistics such as mean and standard deviation were calculated for FSTT at each landmark using IBM Statistical Package for the Social Sciences version 21.0 software (Armonk, New York, United States). The difference between the mean values in the two sexes was compared using Student's t-test and also the differences between the averages of the right and left sides. P value was set as 0.05 at 5% significance level.

RESULTS

Tables 1 and 2 summarize the mean, standard deviation, as well as minimum, maximum and range determined for

each of the 34 anatomical landmarks. For all the inferential statistics, the P value was set as 0.05 at 5% significance level. "T" score from independent t-test and P values for significance level of all the variables are derived and results are tabulated in Tables 3 and 4. Along both right and left sides, a significant difference between the mean values of male and female was noticed at mid-supraorbital margin, alare curvature point, gonion, supracanine, infracanine and midramus. In the remaining landmarks, i.e., mid-infraorbital margin, zygion, supramolar, inframolar and mid-mandibular border, although the mean values differed between the two sexes, the statistical differences could not be established. In general, males

Table 1: Descriptive statistics of midline facial soft tissue thickness (mm) at various craniometric landmarks

Landmarks	Mean	Minimum	Maximum	Range	SD
g	5.11	2.86	9.77	6.91	1.23
n	6.78	1.71	11.16	9.45	1.73
mn	3.98	1.42	7.57	6.15	1.15
rhi	2.35	0.84	4.58	3.74	0.74
sn	13.62	3.69	20.25	16.56	2.77
mp	12.00	3.06	17.24	14.18	2.55
ls	12.15	3.19	19.27	16.08	2.91
li	13.97	4.46	20.12	15.66	3.03
mls	11.42	5.56	18.09	12.53	2.15
pg	11.71	2.83	19.37	16.54	3.31
gn	8.46	1.97	17.68	15.71	3.35
m	5.92	2.29	15.58	13.29	2.29

SD: Standard deviation, g: Glabella, n: Nasion, mn: Midnasal, rhi: Rhinion, sn: Subnasal, mp: Midphiltrum, ls: Labrale superius, li: Labrale inferius, mls: Mentolabial sulcus, pg: Pogonion, gn: Gnathion, m: Menton

Table 2: Descriptive statistics of bilateral facial soft tissue thickness (mm) at various craniometric landmarks

Landmarks	Mean	Minimum	Maximum	Range	SD
Right mso	8.04	4.81	11.91	7.10	1.70
Left mso	7.72	4.74	11.33	6.59	1.63
Right mio	5.72	2.98	10.54	7.56	1.59
Left mio	5.82	3.17	11.37	8.20	1.57
Right acp	9.39	5.41	12.85	7.44	1.74
Left acp	9.73	5.22	14.16	8.94	1.87
Right go	13.99	4.23	32.51	28.28	5.77
Left go	14.13	2.96	30.25	27.29	5.96
Right zy	7.97	3.21	15.13	11.92	2.30
Left zy	7.89	3.62	12.53	8.91	2.20
Right sC	11.91	6.26	19.59	13.33	2.56
Left sC	11.77	5.29	17.73	12.44	2.27
Right iC	13.20	5.96	19.87	13.91	2.88
Left iC	13.10	5.40	21.67	16.27	3.04
Right sM^2	29.88	13.67	41.41	27.74	4.96
Left sM^2	29.56	17.39	40.19	22.80	4.54
Right iM$_2$	26.31	16.91	36.11	19.20	4.48
Left iM$_2$	25.71	14.80	34.87	20.07	4.73
Right mr	20.11	10.66	30.63	19.97	4.62
Left mr	19.99	10.57	31.15	20.58	4.65
Right mmb	12.48	4.59	24.02	19.43	4.78
Left mmb	12.33	4.59	24.70	20.11	4.69

SD: Standard deviation, mso: mid-supraorbital, mio: Mid-infraorbital, acp: Alare curvature point, go: Gonion, zy: Zygion, sC: Supracanine, iC: Infracanine, sM^2: Supramolar 2, iM$_2$: Inframolar 2, mr: Midramus, mmb: Mid-mandibular border
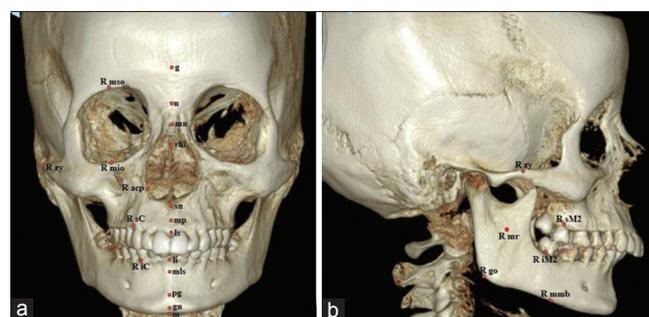

Figure 1: Clinical images of three-dimensional reconstructed skull showing hard tissue landmarks used in the present study. (a) Frontal view showing g: glabella; n: nasion; mn: midnasal; rhi: rhinion; sn: subnasal; mp: midphiltrum; ls: labrale superius; li: labrale inferius; mls: mentolabial sulcus; pg: pogonion; gn: gnathion; m: menton. (b) Right (R) profile view showing mso: mid-supraorbital margin; mio: mid-infraorbital margin; acp: alare curvature point; go: gonion; zy: zygion; sC: supracanine; iC: infracanine; sM2: supramolar 2; iM$_2$: inframolar 2; mr: midramus; mmb: mid-mandibular border

had significantly thicker soft tissues than the females at all landmarks, especially along the midline [Figure 2].

Table 3: Sex-based comparison of midline facial soft tissue thickness (mm) using Student's *t*-test

Landmarks	Males	Females	t	P
g	5.66±1.30	4.56±0.88	4.408	0.000
n	7.74±1.70	5.82±1.12	5.952	0.000
mn	4.34±1.21	3.62±0.98	2.915	0.005
rhi	2.54±0.69	2.15±0.76	2.367	0.020
sn	15.05±2.52	12.20±2.24	5.336	0.000
mp	13.50±2.48	10.50±1.54	6.469	0.000
ls	13.80±2.81	10.49±1.90	6.147	0.000
li	14.96±3.03	12.98±2.71	3.076	0.003
mls	12.22±2.30	10.62±1.66	3.547	0.001
pg	12.87±3.57	10.57±2.59	3.299	0.001
gn	9.72±3.35	7.21±2.88	3.543	0.001
m	6.71±2.73	5.13±1.37	3.219	0.002

g: Glabella, n: Nasion, mn: Midnasal, rhi: Rhinion, sn: Subnasal, mp: Midphiltrum, ls: Labrale superius, li: Labrale inferius, mls: Mentolabial sulcus, pg: Pogonion, gn: Gnathion, m: Menton

Table 4: Sex-based comparison of bilateral facial soft tissue thickness (mm) using Student's *t*-test

Landmarks	Males	Females	t	P
Right mso	8.94±1.52	7.17±1.39	5.387	0.000
Left mso	8.63±1.51	6.83±1.21	5.838	0.000
Right mio	5.97±1.54	5.46±1.62	1.422	0.159
Left mio	6.07±1.40	5.56±1.70	1.484	0.142
Right acp	10.34±1.48	8.45±1.47	5.702	0.000
Left acp	10.68±1.64	8.79±1.60	5.207	0.000
Right go	15.69±6.36	12.30±4.60	2.728	0.008
Left go	15.95±6.74	12.31±4.45	2.841	0.006
Right zy	8.18±2.40	7.75±2.21	0.834	0.407
Left zy	8.29±2.17	7.49±2.19	1.651	0.103
Right sC	13.24±2.53	10.59±1.83	5.355	0.000
Left sC	12.97±2.13	10.57±1.72	5.520	0.000
Right iC	14.06±2.61	12.34±2.92	2.775	0.007
Left iC	13.90±2.92	12.30±2.98	2.423	0.018
Right sM^2	30.58±5.39	29.21±4.48	1.199	0.234
Left sM^2	30.17±5.16	28.97±3.81	1.134	0.261
Right iM$_2$	27.19±4.74	25.43±4.07	1.756	0.083
Left iM$_2$	26.52±4.93	24.91±4.44	1.521	0.132
Right mr	21.93±4.65	18.29±3.87	3.804	0.000
Left mr	22.06±4.64	17.92±3.68	4.424	0.000
Right mmb	13.12±5.37	11.85±4.07	1.194	0.236
Left mmb	13.27±5.10	11.39±4.08	1.825	0.072

mso: mid-supraorbital, mio: Mid-infraorbital, acp: Alare curvature point, go: Gonion, zy: Zygion, sC: Supracanine, iC: Infracanine, sM^2: Supramolar 2, iM$_2$: Inframolar 2, mr: Midramus, mmb: Mid-mandibular border

The mean value and standard deviation between landmarks of the right and left sides in both the sexes were compared, and paired *t*-test was used to test the significant difference between the mean values as shown in Table 5. There were no significant differences between the right and left side measurements except at mid-supraorbital margin and alare curvature point, suggesting no facial asymmetry. Further, correlation test carried out yielded significantly high and positive correlation between right and left sides in both males and females [Table 5].

To understand population diversity, gender-specific comparisons were made between the FSTT of the current study and the Korean data.[15] Statistically significant differences were observed between the two at almost all the anatomical sites [Table 6].

The mean and standard values of tissue depth of South Indian population with the values of other population of the Indian subcontinent were compared as shown in Table 7. Because the landmarks used in other studies varied in terms of number as well as nomenclature, abbreviations and definitions, only those values at the landmarks same or similar to the ones used in the current study were considered for comparison. The values differed among all the studies at all the landmarks. The differences are marked
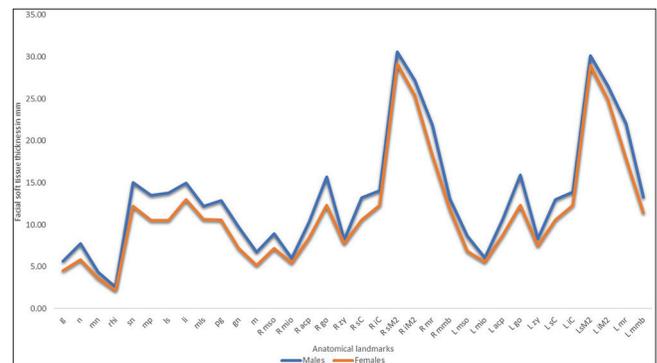

Figure 2: Graph showing gender-based differences in facial soft tissue thickness

Table 5: Comparison and correlation of facial soft tissue thickness (mm) for facial asymmetry

Landmarks	Right	Left	t	P	Correlation	Significance
mso	8.04±1.70	7.72±1.63	3.933	0.000	0.908	0.000
mio	5.72±1.59	5.82±1.57	−0.660	0.511	0.642	0.000
acp	9.39±1.74	9.73±1.87	−3.137	0.002	0.859	0.000
go	13.99±5.77	14.13±5.96	−0.406	0.686	0.871	0.000
zy	7.97±2.30	7.89±2.20	0.617	0.539	0.885	0.000
sC	11.91±2.56	11.77±2.27	0.909	0.366	0.846	0.000
iC	13.20±2.88	13.10±3.04	0.597	0.552	0.859	0.000
sM^2	29.70±4.89	29.56±4.54	0.317	0.752	0.672	0.000
iM$_2$	26.27±4.53	25.82±4.70	1.834	0.071	0.894	0.000
mr	20.11±4.62	19.99±4.65	0.777	0.439	0.953	0.000
mmb	12.48±4.78	12.33±4.69	0.811	0.420	0.936	0.000

mso: mid-supraorbital, mio: Mid-infraorbital, acp: Alare curvature point, go: Gonion, zy: Zygion, sC: Supracanine, iC: Infracanine, sM^2: Supramolar 2, iM$_2$: Inframolar 2, mr: Midramus, mmb: Mid-mandibular border

Table 6: Sex-based comparative analysis of facial soft tissue thickness measurements (mm) of the current study with Hwang et al.[15]

Landmarks	Present study (2018) males (n=40)	Hwang et al. (2012) males (n=50)	P	Present study (2018) Females (n=40)	Hwang et al. (2012) females (n=50)	P
g	5.6±1.3	5.6±0.6	1.000	4.5±0.8	5.3±0.7	<0.001**
n	7.7±1.7	6.4±0.9	<0.001**	5.8±1.1	5.4±0.9	0.067
rhi	2.5±0.6	2.3±0.6	0.120	2.1±0.7	2.2±0.9	0.555
mp	13.5±2.8	12.5±1.1	0.038*	10.5±1.5	10.7±1.4	0.519
ls	13.8±2.8	11.7±2.0	<0.001**	10.4±1.9	9.9±1.7	0.198
li	14.9±3.0	13.0±1.9	0.001**	12.9±2.7	11.6±1.6	0.009*
mls	12.2±2.3	11.6±1.1	0.135	10.6±1.6	10.2±1.1	0.183
pg	12.8±3.5	12.3±1.4	0.399	10.5±2.5	12.0±1.8	0.002*
m	6.7±2.7	8.0±1.5	0.008*	5.1±1.3	6.9±1.5	<0.001**
mso	8.9±1.5	7.2±1.1	<0.001**	7.1±1.3	6.4±1.0	0.006*
mio	5.9±1.5	7.4±1.4	<0.001**	5.4±1.6	7.3±1.3	<0.001**
acp	10.3±1.4	14.3±1.7	<0.001**	8.4±1.4	12.4±1.7	<0.001**
sC	13.2±2.5	11.0±1.0	<0.001**	10.5±1.8	10.3±1.5	0.575
iC	14.0±2.6	12.2±1.5	<0.001**	12.3±2.9	10.8±1.5	0.004*
zy	8.1±2.4	8.1±1.7	1.000	7.7±2.2	8.7±1.4	0.015*
sM^2	30.5±5.3	28.5±2.7	0.034*	29.2±4.4	27.7±3.4	0.080
iM_2	27.1±4.7	21.1±2.8	<0.001**	25.4±4.0	20.3±2.4	<0.001**
go	15.6±6.3	14.3±4.0	0.261	12.3±4.6	12.9±2.3	0.455
mmb	13.1±5.3	7.9±1.7	<0.001**	11.8±4.0	7.7±1.7	<0.001**

*P<0.05; **P<0.01. g: Glabella, n: Nasion, mn: Midnasal, rhi: Rhinion, mp: Midphiltrum, ls: Labrale superius, li: Labrale inferius, mls: Mentolabial sulcus, pg: Pogonion, m: Menton, mso: mid-supraorbital, mio: Mid-infraorbital, acp: Alare curvature point, go: Gonion, zy: Zygion, sC: Supracanine, iC: Infracanine, sM^2: Supramolar 2, iM_2: Inframolar 2, mmb: Mid-mandibular border

Table 7: Comparison of the facial soft tissue thickness means (mm) of the current study to other Indian studies

Landmarks	Kotrashetti and Mallapur[17] (i) Radiographs	Sahni et al.[18] (ii) MRI scans	Kaur et al.[30] (iii) CT scans	Present study (iv) CBCT	P	Multiple comparisons (Tukey's HSD test)
g	5.50±0.93	3.82±0.76	5.01±1.8	5.11±1.23	<0.001*	i versus ii (P<0.001*), i versus iii (P=0.013*), i versus iv (P=0.018*) ii versus iii (P<0.001*), ii versus iv (P<0.001*) and iii versus iv (P=0.9818)
n	5.93±1.56	2.75±0.38	6.11±1.79	6.78±1.73	<0.001*	i versus ii (P<0.001*), i versus iii (P=0.897), i versus iv (P<0.001*) ii versus iii (P<0.001*), ii versus iv (P<0.001*) and iii versus iv (P=0.038*)
rhi	2.21±0.53	2.26±0.35	2.36±2.10	2.35±0.74	<0.001*	i versus ii (P=0.926), i versus iii (P=0.690), i versus iv (P=0.578) ii versus iii (P=0.909), ii versus iv (P=0.879) and iii versus iv (P=1.000)
sn	14.03±1.99	NA	5.49±2.57	13.62±2.77	<0.001*	i versus iii (P<0.001*), i versus iv (P=0.431) and iii versus iv (P<0.001*)
mp	NA	10.08±2.04	11.08±2.81	12.00±2.55	<0.001*	ii versus iii (P=0.029*), ii versus iv (P<0.001*) and iii versus iv (P=0.134)
ls	11.39±2.12	8.74±1.95	8.39±2.69	12.15±2.91	<0.001*	i versus ii (P<0.001*), i versus iii (P<0.001*), i versus iv (P=0.066) ii versus iii (P=0.858), ii versus iv (P<0.001*) and iii versus iv (P<0.001*)
li	13.64±2.35	11.22±0.99	9.04±2.63	13.97±3.03	<0.001*	i versus ii (P<0.001*), i versus iii (P<0.001*), i versus iv (P=0.722) ii versus iii (P<0.001*), ii versus iv (P<0.001*) and iii versus iv (P<0.001*)
pg	10.94±2.05	8.42±1.88	10.84±2.31	11.71±3.31	<0.001*	i versus ii (P<0.001*), i versus iii (P=0.998), I versus iv (P=0.043*) ii versus iii (P<0.001*), ii versus iv (P<0.001*) and iii versus iv (P=0.184)
gn	6.61±1.48	NA	8.73±2.81	8.46±3.35	<0.001*	i versus iii (P<0.001*), i versus iv (P<0.001*) and iii versus iv (P=0.892)
m	NA	5.99±1.67	7.14±3.39	5.92±2.29	<0.001*	ii versus iii (P=0.002*), ii versus iv (P=0.993) and iii versus iv (P=0.006*)

*P is statistically significant. NA: Not available, g: Glabella, n: Nasion, rhi: Rhinion, sn: Subnasal, mp: Midphiltrum, ls: Labrale superius, li: Labrale inferius, pg: Pogonion, gn: Gnathion, m: Menton, MRI: Magnetic resonance imaging, CT: Computed tomography, CBCT: Cone-beam computed tomography

between those derived from the radiographic assessment to the ones from the advanced imaging techniques. However, the measurements obtained from CT and CBCT were comparable and the differences are statistically insignificant at most of the points: glabella, rhinion, midphiltrum, labrale inferius, pogonion and gnathion.

DISCUSSION

FSTT measurements have been recorded using a number of invasive and noninvasive techniques. Needle puncture method employed in the past had certain limitations such as limited subject availability and problems while skin puncture.[16] Feasibility of tissue penetration dictated the selection of anatomical sites. To overcome some of these limitations, various noninvasive imaging modalities such as lateral cephalograms, USG, MRI and CT evolved. Lateral cephalograms[17] reveal only midline FSTT values. While USG analysis is an appropriate alternative especially for large-scale studies,[13] anatomical sites chosen for the measurements are limited. Because it is a real-time imaging, new measurements cannot be incorporated at a later date.[15] Measurement errors are likely due to indentation of facial tissues with the transducer. This compels the investigators to repeat measurements which costs time and effort.[13] Further, transducer orientation will determine the thickness of the tissues.

CT and MRI minimized these limitations.[12,18] Unlike USG, the measurement sites can be added at a later date according to the research requirements and the problems associated with transducer is eliminated. However, patient is in supine position during both the procedures, which results in gravity induced reduction in midline FSTT measurements while increasing the lateral ones.[21]

CBCT system designed specifically for head and neck imaging has emerged as an effective tool for measuring FSTT. The dose of CBCT is almost 100 times less when compared to CT scans[22] ranging from 102 to 298 μsv at lower resolution settings and exposures parameters. The mean effective doses for large and medium FOVs is 212 μSv and 177 μSv, respectively, which is far lower than the effective dose of approximately 860 μSv in CT.[22,23]

CBCT gives a good representation of the facial soft tissues. Farman and Scarfe reported that the clarity in soft tissue definition with CBCT is sufficient to determine air/soft boundaries and also the patient's profile.[24] By integration of flat panel detectors, visualization of soft tissues has further improved.[25]

The scans used in the current study were in the voxel size of 0.3–0.4 mm in accordance with Fourie et al.[16] Small voxel size of 0.2 mm results in a very large surface mesh model, which makes it difficult to process an accurate 3D surface model apart from increasing patient radiation exposure while the use of bigger voxel sizes will cause loss of some relevant details.[26] Patients in the current study were positioned upright with FH plane parallel to the floor to standardize patient positioning. This will avoid gravity-related measurement errors. Although Hoogeveen et al. have demonstrated negligible differences.[27] Munn and Stephan demonstrated that posture variation affect the average FSTT measurements, especially in the cheeks, eyes and nasolabial fold area.[21]

All the hard tissue and their homologous soft tissue landmarks in the present study were identified manually on volume rendered image at first and then was precisely defined on MPR slices for increasing the accuracy. The volume-rendered image was reoriented to make FH plane and transorbital plane horizontal although Gupta et al. opined that such reorientations does not enhance the precision of landmark plotting.[28] CBCT allows clinically accurate and reliable 3D linear measurements of the craniofacial complex[29] and allows addition of new parameters postscan unlike USG.[15] Both hard and its homologous soft tissue images can be visualized simultaneously. The 3D reconstructions along with

transplanar cross-sections help in accurate identification of the landmark.[28]

The present study showed significantly higher soft tissue thickness means in males as large as up to 2–3 mm compared to the females at all the midline and certain bilateral (mid-supraorbital margin, alare curvature point, gonion, supracanine, infracanine and mid-ramus) landmarks which correspond to nose–lip and the mandibular angle areas. De Greef et al.[13] on Caucasians and Utsuno et al.[14] on Japanese children observed a similar pattern. This implies that soft tissues in the lip areas are distinctly thicker in men than in women, irrespective of the race. However, Stephan and Simpson insisted that this difference is of little practical implications during craniofacial reconstruction.[20]

To evaluate facial asymmetry, FSTT measurements of the right side were compared with the left. The differences were negligible and insignificant at all the landmarks except mid-supraorbital margin and alare curvature point. The differences were below 0.4 mm and never exceeded 1.2 mm. Researchers with similar results have chosen either to measure FSTT only on the right side of the or to average the bilateral values.[12,13,15]

To evaluate racial variations in FSTT values as have been reported in the literature,[14,19] the data of the present study were compared with the mean values of the Korean population.[15] These two datasets were comparable as both had similar sample size and both used CBCT for measurements. Significant differences in FSTT values were observed at 11–13 landmarks in both the genders emphasizing interpopulation variations in the FSTT and consequently the need for population-specific datasets. Stephan and Simpson opine that such differences occur due to the noise in the data created by measurement errors.[20]

To understand whether the choice of technique affects the measurements, the data of the current study were compared with three other Indian studies[17,18,30] wherein the researchers have used various noninvasive techniques such as lateral cephalogram,[17] MRI[18] and CT.[30] The midline FSTT values of all the four studies differed from one another, the differences being statistically significant between the radiographic study[17] and all the other three. In spite of lateral cephalograms clearly demonstrating the profile soft tissue outlines and facilitating midline measurements, the accuracy of 2D radiographic techniques is limited when compared to the advanced imaging owing to technique related errors such as superimposition. On the contrary, the differences between CT[30] and CBCT

(current study) derived values are negligible and statistically insignificant at majority of the landmarks. CBCT provides high-quality images at a lower radiation dose using less expensive equipment. In addition, cases are not in supine position during the procedure unlike CT, which will eliminate gravity-induced effects on the FSTT values.[21]

CONCLUSION

Using CBCT scans, FSTT averages for South Indian Adults were obtained. Males had significantly thicker facial tissues than females. Negligible differences were noted in the soft tissue thickness between the right and left sides of the face. The measurements obtained in this study can be used as a database for the forensic facial reconstruction of South Indian adults. The values may also find its applications in archeology, maxillofacial and plastic reconstructive surgeries.

Conflicts of interest
There are no conflicts of interest.

REFERENCES

1. Scarfe WC, Farman AG. What is cone-beam CT and how does it work? Dent Clin North Am 2008;52:707-30, v.
2. Goldman LW. Principles of CT and CT technology. J Nucl Med Technol 2007;35:115-28.
3. Scarfe WC, Li Z, Aboelmaaty W, Scott SA, Farman AG. Maxillofacial cone beam computed tomography: Essence, elements and steps to interpretation. Aust Dent J 2012;57 Suppl 1:46-60.
4. Miracle AC, Mukherji SK. Conebeam CT of the head and neck, part 2: Clinical applications. AJNR Am J Neuroradiol 2009;30:1285-92.
5. Pittayapat P, Bornstein MM, Imada TS, Coucke W, Lambrichts I, Jacobs R. Accuracy of linear measurements using three imaging modalities: Two lateral cephalograms and one 3D model from CBCT data. Eur J Orthod 2015;37:202-8.
6. Brogdon BG. The scope of forensic radiology. Clin Lab Med 1998;18:203-40.
7. Ruder TD, Kraehenbuehl M, Gotsmy WF, Mathier S, Ebert LC, Thali MJ, et al. Radiologic identification of disaster victims: A simple and reliable method using CT of the paranasal sinuses. Eur J Radiol 2012;81:e132-8.
8. Thali MJ, Yen K, Vock P, Ozdoba C, Kneubuehl BP, Sonnenschein M, et al. Image-guided virtual autopsy findings of gunshot victims performed with multi-slice computed tomography and magnetic resonance imaging and subsequent correlation between radiology and autopsy findings. Forensic Sci Int 2003;138:8-16.
9. Wilkinson C. Facial reconstruction – Anatomical art or artistic anatomy? J Anat 2010;216:235-50.
10. Stephan CN. Facial approximationation and craniofacial superimposition. In: Smith C, editor. Encyclopedia of Global Archeology. New York: Springer Science + Business Media; 2014. p. 2721-9.
11. Tilotta F, Richard F, Glaunès J, Berar M, Gey S, Verdeille S, et al. Construction and analysis of a head CT-scan database for craniofacial reconstruction. Forensic Sci Int 2009;191:112.e1-12.
12. Thiemann N, Keil V, Roy U. In vivo facial soft tissue depths of a modern adult population from germany. Int J Legal Med 2017;131:1455-88.
13. De Greef S, Claes P, Vandermeulen D, Mollemans W, Suetens P, Willems G. Large-scale in vivo caucasian facial soft tissue thickness database for craniofacial reconstruction. Forensic Sci Int 2006;159 Suppl 1:S126-46.
14. Utsuno H, Kageyama T, Uchida K, Yoshino M, Miyazawa H, Inoue K. Facial soft tissue thickness in Japanese children. Forensic Sci Int 2010;199:109.e1-6.
15. Hwang HS, Park MK, Lee WJ, Cho JH, Kim BK, Wilkinson CM. Facial soft tissue thickness database for craniofacial reconstruction in korean adults. J Forensic Sci 2012;57:1442-7.
16. Fourie Z, Damstra J, Gerrits PO, Ren Y. Accuracy and reliability of facial soft tissue depth measurements using cone beam computer tomography. Forensic Sci Int 2010;199:9-14.
17. Kotrashetti VS, Mallapur MD. Radiographic assessment of facial soft tissue thickness in South Indian population – An anthropologic study. J Forensic Leg Med 2016;39:161-8.
18. Sahni D, Sanjeev, Singh G, Jit I, Singh P. Facial soft tissue thickness in Northwest Indian adults. Forensic Sci Int 2008;176:137-46.
19. Bulut O, Sipahioglu S, Hekimoglu B. Facial soft tissue thickness database for craniofacial reconstruction in the Turkish adult population. Forensic Sci Int 2014;242:44-61.
20. Stephan CN, Simpson EK. Facial soft tissue depths in craniofacial identification (part I): An analytical review of the published adult data. J Forensic Sci 2008;53:1257-72.
21. Munn L, Stephan CN. Changes in face topography from supine-to-upright position-and soft tissue correction values for craniofacial identification. Forensic Sci Int 2018;289:40-50.
22. Ludlow JB, Ivanovic M. Comparative dosimetry of dental CBCT devices and 64-slice CT for oral and maxillofacial radiology. Oral Surg Oral Med Oral Pathol Oral Radiol Endod 2008;106:106-14.
23. Ludlow JB, Timothy R, Walker C, Hunter R, Benavides E, Samuelson DB, et al. Effective dose of dental CBCT-a meta analysis of published data and additional data for nine CBCT units. Dentomaxillofac Radiol 2015;44:20140197.
24. Farman AG, Scarfe WC. Development of imaging selection criteria and procedures should precede cephalometric assessment with cone-beam computed tomography. Am J Orthod Dentofacial Orthop 2006;130:257-65.
25. Heiland M, Pohlenz P, Blessmann M, Habermann CR, Oesterhelweg L, Begemann PC, et al. Cervical soft tissue imaging using a mobile CBCT scanner with a flat panel detector in comparison with corresponding CT and MRI data sets. Oral Surg Oral Med Oral Pathol Oral Radiol Endod 2007;104:814-20.
26. Hassan B, Couto Souza P, Jacobs R, de Azambuja Berti S, van der Stelt P. Influence of scanning and reconstruction parameters on quality of three-dimensional surface models of the dental arches from cone beam computed tomography. Clin Oral Investig 2010;14:303-10.
27. Hoogeveen RC, Sanderink GC, Berkhout WE. Effect of head position on cephalometric evaluation of the soft-tissue facial profile. Dentomaxillofac Radiol 2013;42:20120423.
28. Gupta A, Kharbanda OP, Balachandran R, Sardana V, Kalra S, Chaurasia S, et al. Precision of manual landmark identification

between as-received and oriented volume-rendered cone-beam computed tomography images. Am J Orthod Dentofacial Orthop 2017;151:118-31.

29. Berco M, Rigali PH Jr., Miner RM, DeLuca S, Anderson NK, Will LA. Accuracy and reliability of linear cephalometric measurements from cone-beam computed tomography scans of a dry human skull. Am J Orthod Dentofacial Orthop 2009;136:17.e1-9.

30. Kaur K, Sehrawat JS, Bahadur R. Sex dependent variations in craniofacial soft-tissue thicknesses estimated from MRI and CT scans: A pilot study based on Northwest Indian subjects. Int J Diagn Imaging 2017;4:47.